ELSEVIER

Biophysical Chemistry 122 (2006) 43–49

Biophysical Chemistry

http://www.elsevier.com/locate/biophyschem

Docking studies of Nickel-Peptide deformylase (PDF) inhibitors: Exploring the new binding pockets

Qiang Wang [a], Datong Zhang [b], Jianwu Wang [b], Zhengting Cai [a,*], Weiren Xu [c]

[a] *Institute of Theoretical Chemistry, Shandong University, Jinan 250100, China*
[b] *Institute of Organic Chemistry, Shandong University, Jinan 250100, China*
[c] *Tianjin Institute of Pharmaceutical Research, Tianjin 300193, China*

Received 26 December 2005; received in revised form 13 February 2006; accepted 16 February 2006
Available online 6 March 2006

Abstract

The binding modes of a series of known activity inhibitors docking to Peptide deformylase (PDF) have been studied using molecular docking software AutoDock3.0.5. In this study, good correlation ($R^2=0.894$) between calculated binding energies and experimental inhibitory activities is obtained. We find that some shallow pockets near the known active pocket are very important which can accommodate the side-chains of the inhibitor. Moreover, a new binding pocket is also explored. All these may provide something useful for designing the potent inhibitors.
© 2006 Elsevier B.V. All rights reserved.

Keywords: Peptide deformylase (PDF) inhibitor; Binding pocket; Docking; Protein–ligand interaction

1. Introduction

In recent years, with the changing of environments, the bacterial infections emerge rapidly and have become a serious threat to respiratory and skin infections [1]. New classes of antibacterial agents with high activities are required. It is not surprising that antibacterial drug discovery efforts are now focused on identifying targets. One of such targets receiving widespread interests from theoretical and pharmic researchers was Peptide deformylase (PDF) [2,3], a highly conserved metalloenzyme, was responsible for the removal of the formyl group for the majority of bacterial proteins [4]. The *Escherichia coli* enzyme used Fe^{2+} and nearly retained its activity on substitution of the metal ion by Ni^{2+} [5]. The structure of the catalytically active enzyme in the nickel-bound form (PDF-Ni) at different resolutions in complexes was described [6]. Many structure–activity relationship (SAR) analyses about the PDF inhibitors were also reported [7–10].

In this paper, the simulation results of the inhibitors of using computational drug design are given. This approach utilizes structural information of the substrate binding pocket of the target enzyme obtained from examining the available crystal structure of the target enzyme. Then small molecule inhibitors will be proposed by examining their interactions with the amino acid residues of the substrate-binding pocket of the target enzyme.

Two representative examples in the Nickel-PDF retrieved from the RSCB Protein Data Bank [11] are 1G2A and 1G27 for their extensive researches. Firstly, we want to analyze the interactions between the receptor and inhibitors to explore their binding modes. According to our knowledge, simulation of the 1G2A and 1G27 complexes using AutoDock software [12] has not been reported in the literature by far. 1G2A and 1G27 have the same receptor and X-ray structures of them are available. To be consistent in the subsequent docking studies of other compounds, only the protein structure of 1G2A is used because it (1.75 Å) has a better resolution than 1G27 (2.10 Å) [11].

2. Compounds and computational methodology

The Sybyl 7.0 package [13] is used to prepare the docking files. For the protein, A chain is kept, while the B and C chains are deleted; the water and ligand are also removed except for the Nickel ion in the active site. Polar hydrogen atoms are added

* Corresponding author. Tel.: +86 531 88365746; fax: +86 531 88564464.
E-mail address: zhtcai@sdu.edu.cn (Z. Cai).

0301-4622/$ - see front matter © 2006 Elsevier B.V. All rights reserved.
doi:10.1016/j.bpc.2006.02.009

and Kollman charges are assigned. AutoDock3.0.5 is used for all docking calculations. For docking a grid spacing of 0.375 Å and 60 × 60 × 60 number of points are created for protein. For the Lamarckian genetic algorithm (LGA) is more efficient than others, it is applied to search the conformational and orientational space of the inhibitors while keeping the protein structures rigid. For those structures which lack crystallographic data in Table 1, the complexes are generated and manually adjusted to be as similar as possible to their crystal conformation. All amide bonds are considered as non-rotatable. For all dockings, 50 independent runs with a maximum number of 2,000,000 energy evaluations, a mutation rate of 0.02 and a crossover rate of 0.8 are used.

Metal ions are modeled in AutoDock by Amber force field potentials [14]. The Ni initial parameters (are set as $r = 1.170$ Å, $q = +2.0$ and van der Waals well depth of 0.100 kcal/mol) reported by Musiani [15] as the Autodock default values.

A lot of natural or synthetic compounds with inhibitory activities have been so far reported [16–23]. PDF protease bound with 17 inhibitors like a substrate is used as the starting point for the modeling study, and the congruent activity data of these inhibitors are available [16–23], reported in Table 1.

Table 1
PDF inhibitory activity of compounds **1**–**17**

Compound	Structure	IC_{50} (nM)	Compound	Structure	IC_{50} (nM)
1	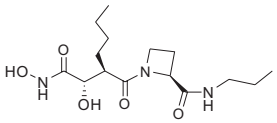	6.7	**10**	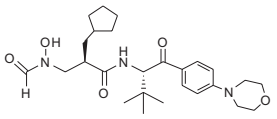	2
2	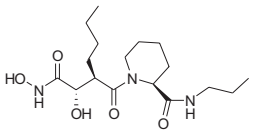	6.7	**11**	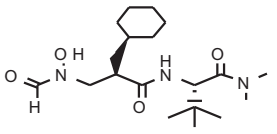	6
3	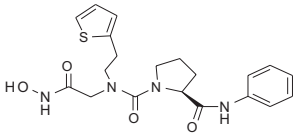	2	**12**	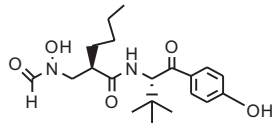	8
4	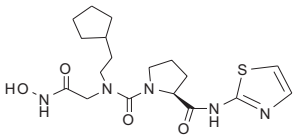	16	**13**	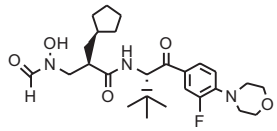	0.6
5	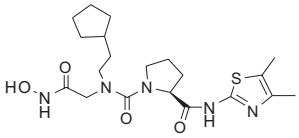	2	**14**	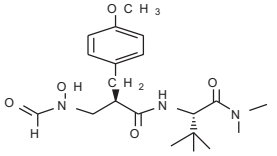	200
6	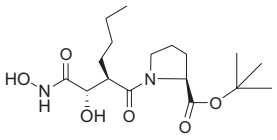	1	**15**	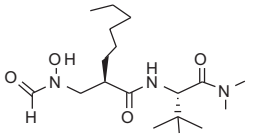	30
7	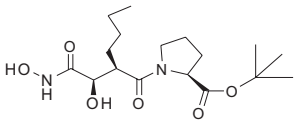	6	**16**	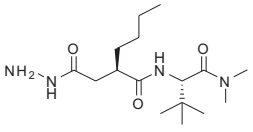	200
8	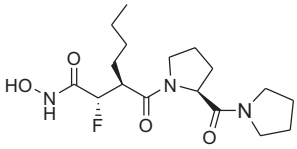	20	**17**	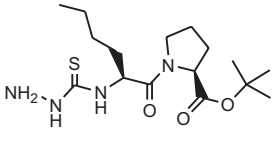	590
9	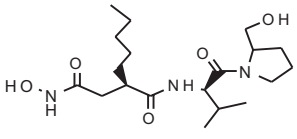	10			

According to the binding groups with metal Ni, these inhibitors can be classed three types: hydroxamate, *N*-formylhydroxylamine and other kinds of compounds. Hydroxamate and *N*-formylhydroxylamine are the derivatives of the ligands of 1G2A and 1G27 complex, respectively. As for other kinds of compounds, low-activity leads them to little extensive applications.

3. Results and discussion

The best docked configurations for the ligands in Table 1 are used to calculate interaction energies. The results reveal that all the studied 1G2A derivatives can dock into the PDF enzyme. The estimated free energies of binding are plotted against the experimental inhibitory activities in Fig. 1 for all the compounds. AutoDock results are in good agreement with the experimental values, which demonstrates a good linear relationship and the trend can indicate that the docking program produces reasonable binding modes.

As part of our efforts to develop new PDF inhibitors, we investigate the binding modes of PDF inhibitors using AutoDock. The binding site in Ni-PDF is described as in Ref. [24]. Our main interest is how to use the binding site to elucidate the interactions which contribute to the binding affinity of new inhibitors; such information is necessary for the further design of more potent inhibitors. Among these 17 compounds (including 1G2A ligand), 15 compounds show significant inhibitory activity against the PDF protease.

3.1. Docking to the hydroxamate

Compounds **1**–**9** in Table 1 belong to hydroxamate and they have the same functional group HONHCO– coordinated to metal Ni. Compared to **9** (original ligand of 1G2A), **1** and **2** are similar to each other. Four- to six-membered cyclicamino groups in the P2′ position shield the neighboring amide nitrogen and reduce hydrogen bonding to bulk solvent [25]. It is worth noting that the hydroxyl group on the side-chain of compounds **1** and **2** is important in increasing binding affinity. It forms H-bond with the residues of the receptor, and the binding affinity between them is increased. For compound **1**, the hydroxyl group of HONHCO is hydrogen bonded to the amide hydrogen of LEU91, and the bonding distance between them is 2.60 Å. For compound **2**, hydrogen bond (2.20 Å) is also made by the carbonyl oxygen of GLY45 and the hydroxyl hydrogen of the HONHCO–. So we can say that if the hydroxyl group is linked to the side-chain of **3** like **1** and **2**, the activity of **3** will be improved obviously. But if the *n*-butyl is changed to other rings, for example **3** and **5**, the activity will also be increased. On the other hand, for **5** the methyl is electron-donating group which increases the electron density of sulfur and nitrogen so that they can form the hydrogen bond with the residues. At the same time, the cyclopentylmethyl on the side-chain has strong hydrophobic interaction with the residues, which can be seen from example **10**. If the nitrogen atom of *n*-propyl amino of **1** is changed to oxygen, PDF inhibitory activity will be improved for the oxygen atom belonging to electron-withdrawing substituents. **6** is such an example, oxygen atom forms the hydrogen bond (2.82 Å) with the amine hydrogen of CYS90, and IC_{50} is greatly decreased to

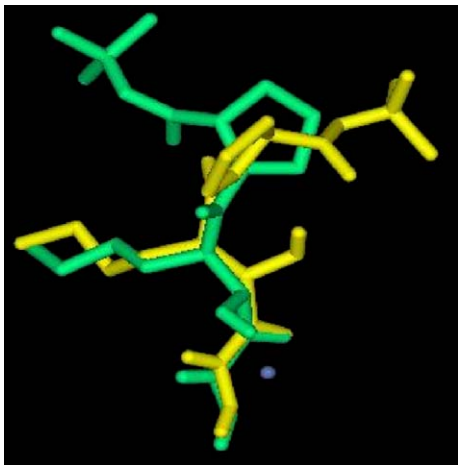

Fig. 2. Comparison of the AutoDock conformations of **6** (yellow) and **7** (green). The metal ion is shown as a blue sphere. (For interpretation of the references to color in this figure legend, the reader is referred to the web version of this article.)

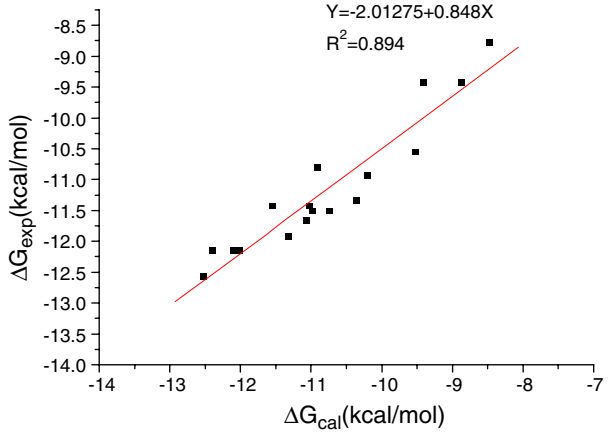

Fig. 1. Linear regression of estimated free energy of binding from AutoDock vs. experimental values derived from IC_{50}.

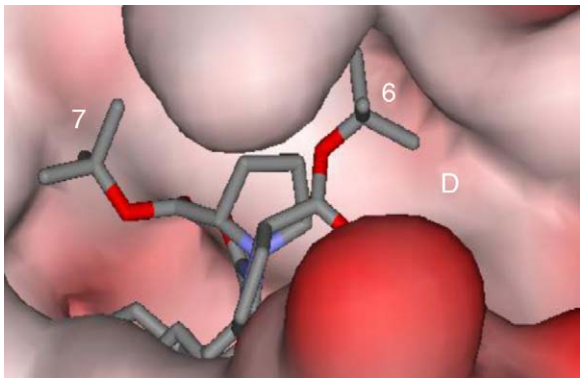

Fig. 3. The isopropyls of **6** and **7** point to different pockets. D is a new binding pocket. Solvent-accessible protein surface is colored by electrostatic potential.

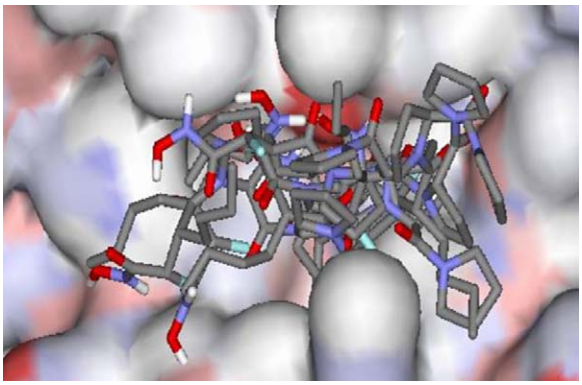

Fig. 4. Docked conformations of **8** occupy the new binding pocket. The protein surface is colored by atom charge.

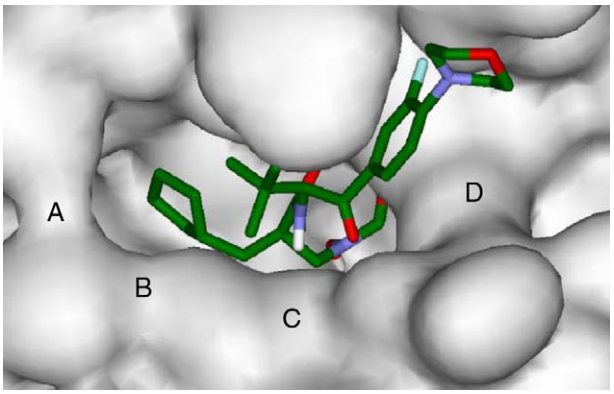

Fig. 6. View of surface and **13** docked into the active site of PDF is shown as a stick.

1 nM, so –COO– group is better than –CONH–. **6** and **7** are isomerous with each other in Fig. 2, but their activities are much different, the main season is that the hydroxyl group in the side-chain plays an important role. For **6**, hydroxyl group is trans to *n*-butyl; the hydrogen bond is formed between the CHO of **6** and the amine hydrogen of LEU91, which is 2.74 Å. For **25**, hydroxyl group is cis to *n*-butyl, the distance between hydroxyl oxygen and amine hydrogen of ILE44 is 2.83 Å. Although the hydrogen bond is almost equal, the hydroxyl group interacts with different residues, the isopropyls point to different hydrophobic cavity. From Fig. 3 we can see that the isopropyl of **6** can bind strongly with the residues in the new pocket D, this binding mode decreases IC_{50} to 1 nM, pocket D is necessary in designing new inhibitors. Although an aromatic ring [19] was added in the P3′ position which decreased the binding constant of PDF, the pocket D was not pointed out, the existence of pocket D just explains why people want to modify the side-chain of PDF in the P3′ position.

Of all the docked ligands, 14 of them can be docked into the known active site of 1G2A. This supports our initial hypothesis that the ligands will dock into the pocket of a protein in a manner similar to the way of 1G2A crystal complex. The most dockings occur on the core domain of protein, but the other two inhibitors are docked to another pocket. In light of the fact that the deformylase active site residues are hydrophobic, they should be directed toward a pocket composed of hydrophobic residues. The residues on one side of the pocket in Fig. 4 include PRO19, ARG113, ILE57, VAL59, VAL16, VAL138, MET134, CYS129, LYS140, GLU64 and TYR145. Those on the other side are ARG109, ALA110, PHE118, GLU76, LEU77, LYS80, ASO123 and GLD83. Of all 50 completed runs, compounds **3** and **8** have 6 and 8 conformations occupying the pocket, respectively. It is interesting that the cyclopentanes are almost directly to the right of the pocket. Although it is unlikely that far from the active site would allow this binding mode, this result suggests that the pocket could be exploited to gain additional binding site in the design of new types of PDF inhibitors. These intimate hydrophobic interactions between the protein and the inhibitor no doubt contribute in an important way to the binding affinity of the inhibitor. Although the activities of **3** and **8** are not high, perhaps the results could provide a helpful preference for designing the potential new inhibitors.

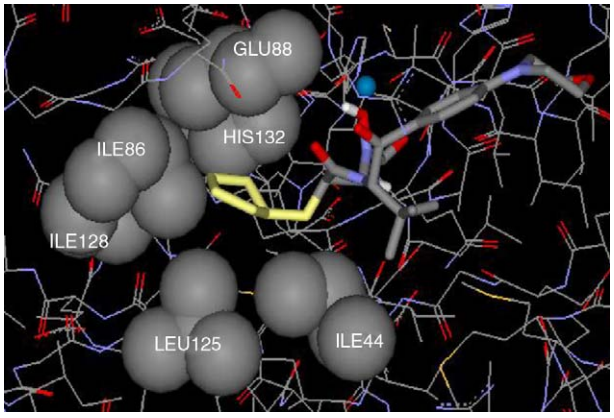

Fig. 5. The cyclopentylmethyl in yellow of **10** insets a hydrophobic pocket of the receptor. The residues and **10** are shown in CPK and stick, respectively, and the hydrogen in the receptor are hidden. The blue ball represents the position of the Nickel ion. (For interpretation of the references to color in this figure legend, the reader is referred to the web version of this article.)

3.2. Docking with N-formylhydroxylamine

These compounds include **10**–**15** in Table 1; their common group in these compounds is HCO–NOH. The activities of these inhibitors are strongly influenced by the nature of the substituent in the P1′ position. Comparing **12** with **10**, the ring on the side-chain has more steric effect than the aliphatic groups. The substituents in P1′ such as *n*-butyl and cyclopentylmethyl,

Table 2
Comparison of the bond distance (Å) and IC_{50} (nM) among **9**, **16** and **17**

9			**16**			**17**		
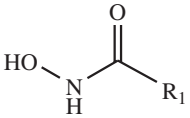			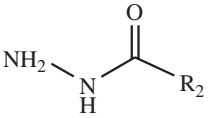			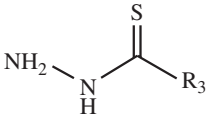		
Ni…OH	Ni…OC	IC_{50}	Ni…NH_2	Ni…OC	IC_{50}	Ni…NH_2	Ni…SC	IC_{50}
2.30	2.20	10	2.94	2.74	200	5.73	6.43	590

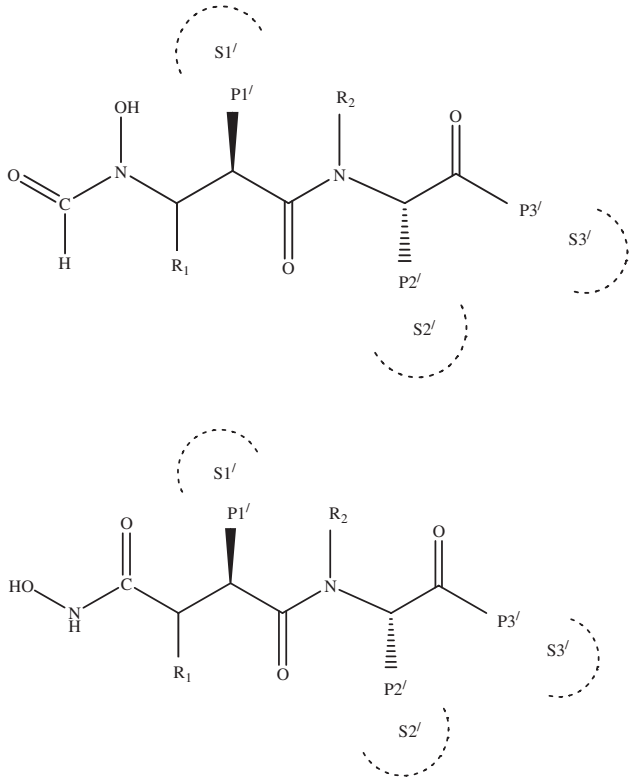

Fig. 7. General structures of hydroxamate and *N*-formylhydroxylamine derivatives. R_1, R_2, P1′, P2′ P3′ are the groups which may be modified and S1′, S2′, S3′ are hydrophobic cavities of the PDF enzyme.

provide potent PDF inhibitors that displayed promising antibacterial activities [26]. For **10**, cyclopentane insets a hydrophobic cavity [27] in Fig. 5 which is composed of ILE44, ILE86, GLU88, LEU125, ILE128 and HIS132, this cavity plays a role of fixing the inhibitor. Modifications adjacent to the metal binding group and to the *n*-butyl substituent are limited due to the steric requirements for binding the active site metal and size of the hydrophobic S1′ cavity [28]. Previous study indicated that an *n*-pentyl group can replace methionine at the P1′ site of the PDF substrate [29]; *n*-pentyl chain was well-accommodated but may be slightly long for the S1′ cavity of the enzyme. In fact, cyclopentylmethyl has not approached ILE86 and ILE128; maybe those groups like cyclopentylethyl are bigger and more fit to fill in the S1′ cavity.

In the P2′ position, the *tert*-butyl is exposed to solvent but does make van der Waals interactions with the residue GLY89. Molecular surface visualization shows that there are four shallow pockets (A, B, C and D) on the protein surface in Fig. 6. The residues in pocket A are HIS132, GLN131, ILE128 and CYS129. B is shallow and has little residues including CYS129, LEU72 and ILE44. Pocket C is composed of ILE44, GLY45, GLY43 and LEU46. D has most residues such as LEU141, SER92, GLU95, PRO94, GLN96, LEU91, CYS90, LEU46 and aromatic groups can be accommodated. Enzyme inhibiting potency is strongly increased by converting the diethylamine of **11** into benzene derivatives. Atom F is hydrogen bonded with amine hydrogen of GLY95, and the bond length is 1.70 Å. The enzyme should be able to accommodate a number of different groups in this position. Supposed that big groups like phenyl are also linked to the B, C and D pockets, interactions of these pockets with the aromatic groups could enhance the binding ability. A range of substituents and functional groups are tolerated by PDF in the P2′ and P3′ positions, which are largely exposed to solvent, but the existence of these pockets requires us that all four pockets should be considered when designing the new inhibitors.

3.3. Docking other compounds

In the complex of compound **9**, the oxygen nickel binding distances are 2.30 Å (to the nitrogen-bound oxygen atom) and 2.20 Å (to the carbonyl oxygen atom), respectively. For **16** and **17**, with the coordinating groups changing, the inhibitory activities are also decreased. For example, in the aspect of the coordination bond, the bond of **17** is longer than that of **9** and **16**, and its IC_{50} is only 590 nM. To compare the three docked moleculars (**9**, **16**, **17**), their binding conformations obtained from the AutoDock run could be seen from Table 2. So when we choose the inhibitor for PDF enzyme, the coordinating group NH_2NHCO and NH_2NHCS should not be considered.

3.4. Designing of new inhibitors

Our fundamental interests in PDF systems come from its potential as a target for antibacterial chemotherapy. Indeed, the studies of these examples offer certain guidelines for the design of high-affinity PDF inhibitors. Three main interactions exist in

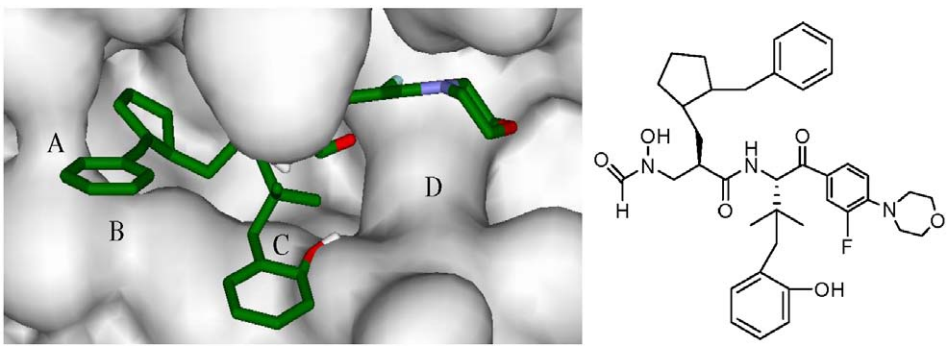

Fig. 8. New proposed inhibitor docked to the PDF surface.

PDF-inhibitor complexes, which are bidentate coordination to Ni, hydrogen bond with the residues, hydrophobic interaction in the P1′ position. When considering the coordinating group, HONHCO and CHONHNOH are preferred in Fig. 7. The substituents in P1′ such as *n*-butyl and cyclopentylmethyl make the inhibitors display promising antibacterial activity. The groups closing to the shallow pockets should be electron-withdrawing substituents or derivatives of phenyl. Aromatic rings in the P2′ and P3′ positions strongly improve affinity between PDF and inhibitor. The P3′ side-chain makes hydrophobic contacts with the shallow pocket D near the active site. R_1 may be atom F, $-NH_2$ or $-OH$, R_2 is four- to six-membered cyclic amino groups. In addition, large aromatic groups are needed to fill in hydrophobic pockets A, B, C and D.

More importantly, we also found a new binding pocket, where the inhibitors lay there as shown in Fig. 4. In the following discussion, the pocket is not revolved, although the activities of **3** and **8** are not high; the pocket may be helpful in designing stronger specifically binding ligands for PDF. From the results discussed above, a class of structure with branched aromatic groups and hydroxyl group can be proposed.

From this finding, it is clear that one of the design strategies for PDF inhibitors is to utilize four pockets on the PDF surface to accommodate the side-chain. Four pockets are particularly interesting in how they contribute to enhance the inhibitory activities, which are important in the interaction that could potentially be exploited for drug development. After the groups in the P1′ and P2′ positions being modified, the new derivative of *N*-formylhydroxylamine in Fig. 8 can be designed.

Although the inhibitory activity of our designed structure in Fig. 8 is unknown, we think that these shallow pockets can enhance the binding affinity between the ligand and receptor. Certainly, we only consider P1′ and P2′; the groups in positions R_1, R_2 and P3′ can also be changed. In other words, our designed molecule is only an example; more compounds like this according to our suggestions can be rebuilt. But we hope our efforts can provide useful information for the experimental researchers to design more potential activities inhibitors.

4. Conclusions

The binding modes of a series of PDF inhibitors are explored using molecular docking software. New shallow pockets near known active pocket are found, which are A, B, C and D pockets, respectively. These pockets can accommodate side-chain of inhibitors such as aromatic groups, which could enhance the binding affinity. In addition, a new binding pocket coming from the docking of **3** and **8** is found; although its properties are not clear, this binding region could increase the possibilities of docking the inhibitors to receptor. All these may be useful in both theory and experiments.

Acknowledgements

The authors acknowledge the supports of National Key Basic Research Priority Program (2003CCA027), Grant No. 20573064 from the National Natural Science Foundation of China and Ph.D. Special Research Foundation of Chinese Ministry of Education.

References

[1] A. Tomasz, Multiple-antibiotic-resistant pathogenic bacteria — a report on the Rockefeller University workshop, N. Engl. J. Med. 330 (1994) 1247–1251.
[2] D. Pei, Peptide deformylase: a target for novel antibiotics? Emerg. Ther. Targets 5 (2001) 23–40.
[3] Z. Yuan, J. Trias, R.J. White, Deformylase as a novel antibacterial target, Drug Discov. Today 6 (2001) 954–961.
[4] J.M. Adams, M.R. Capecchi, N-formylmethionyl-sRNA as the initiator of protein synthesis, Proc. Natl. Acad. Sci. 55 (1966) 147–155.
[5] D. Groche, A. Becker, I. Schlichting, W. Kabsch, S. Schultz, A.F. Wagner, Isolation and crystallization of functionally competent *Escherichia coli* Peptide deformylase forms containing either Iron or Nickel in the active site, Biochem. Biophys. Res. Commun. 246 (1998) 342–346.
[6] A. Becker, I. Schlichting, W. Kabsch, S. Schultz, A.F.V. Wagner, Structure of Peptide deformylase and identification of the substrate binding site, J. Biol. Chem. 273 (1998) 11413–11416.
[7] S.J. Davies, A.P. Ayscough, R.P. Beckett, R.A. Bragg, J.M. Clements, S. Doel, C. Grew, S.B. Launchbury, G.M. Perkins, L.M. Pratt, H.K. Smith, Z. M. Spavold, S.W. Thomas, R.S. Todd, M. Whittaker, Structure–activity relationships of the Peptide deformylase inhibitor BB-3497: modification of the methylene spacer and the P1′ side chain, Bioorg. Med. Chem. Lett. 13 (2003) 2709–2713.
[8] S.K. Grant, B.G. Green, J.W. Kozarich, Inhibition and structure–activity studies of methionine hydroxamic acid derivatives with bacterial Peptide deformylase, Bioorg. Chem. 29 (2001) 211–222.
[9] H.K. Smith, R.P. Beckett, J.M. Clements, S. Doel, S.P. East, S.B. Launchbury, L.M. Pratt, Z. Spavold, W. Thomas, R.S. Todd, M. Whittaker, Structure–activity relationships of the Peptide deformylase inhibitor BB-3497: modification of the metal binding group, Bioorg. Med. Chem. Lett. 12 (2002) 3595–3599.
[10] S.J. Davies, A.P. Ayscough, R.P. Beckett, J.M. Clements, S. Doel, L.M. Pratt, Z.M. Spavold, S.W. Thomas, M. Whittaker, Structure–activity relationships of the Peptide deformylase inhibitor BB-3497: modification of the P2′ and P3′ side chains, Bioorg. Med. Chem. Lett. 13 (2003) 2715–2718.
[11] RSCB Protein Data Bank, web address: http://www.rscb.org/pdb/.
[12] Web address: http://www.scripps.edu/mb/olson/doc/autodock/.
[13] SYBYL modeling software, V7.0, Tripos Associates.
[14] S.J. Weiner, P.A. Kollman, D.A. Case, U.C. Singh, C. Ghio, G. Alagona, S. Profeta, P. Weiner, A new force field for molecular mechanical simulation of nucleic acids and proteins, J. Am. Chem. Soc. 106 (1984) 765–784.
[15] F. Musiani, E. Arnofi, R. Casadio, S. Ciurli, J. Biol. Inorg. Chem. 6 (2001) 300–314.
[16] C. Apfel, D.W. Banner, D. Bur, M. Dietz, C. Hubschwerlen, H. Locher, F. Marlin, R. Masciadri, W. Pirson, H. Stalder, 2-(2-oxo-1,4-dihydro-2H-quinazolin-3-yl)- and 2-(2,2-dioxo-1,4-dihydro-2H- $2\lambda^6$-benzo[1,2,6]thiadiazin-3-yl)-N-hydroxy-acetamides as potent and selective Peptide deformylase inhibitors, J. Med. Chem. 44 (2001) 1847–1852.
[17] M.H. Howard, T. Cenizal, S. Gutteridge, W.S. Hanna, Y. Tao, M. Totrov, V. A. Wittenbach, Y.J. Zheng, A novel class of inhibitors of Peptide deformylase discovered through high-throughput screening and virtual ligand screening, J. Med. Chem. 47 (2004) 6669–6672.
[18] M.M.K. Jayasekera, A. Kendall, R. Shammas, M. Dermyer, M. Tomala, M.A. Shapiro, T.P. Holler, Novel nonpeptidic inhibitors of Peptide deformylase, Arch. Biochem. Biophys. 381 (2000) 313–316.
[19] T. Meinnel, L. Patiny, S. Ragusa, S. Blanquet, Design and synthesis of substrate analogue inhibitors of Peptide deformylase, Biochemistry 38 (1999) 4287–4295.
[20] D.Z. Chen, D.V. Patel, C.J. Hackbarth, W. Wang, G. Dreyer, D.C. Young, P.S. Margolis, C. Wu, Z.J. Ni, J. Trias, R.J. White, Z. Yuan, Actinonin, a

naturally occurring antibacterial agent, is a potent deformylase inhibitor, Biochemistry 39 (2000) 1256–1262.
[21] R.N. Jones, T.R. Fritsche, H.S. Sader, Antimicrobial spectrum and activity of NVP PDF-713, a novel peptide deformylase inhibitor, tested against 1837 recent Gram-positive clinical isolates, Diagn. Microbiol. Infect. Dis. 49 (2004) 63–65.
[22] R.N. Jones, H.S. Sader, T.R. Fritsche, Antimicrobial activity of LBM415 (NVP PDF-713) tested against pathogenic *Neisseria* spp. (*Neisseria gonorrhoeae* and *Neisseria meningitidis*), Diagn. Microbiol. Infect. Dis. 51 (2005) 139–141.
[23] P.S. Chae, M.S. Kim, C.S. Jeung, S.D. Lee, H. Park, S. Lee, J. Suh, Peptide-cleaving catalyst selective for Peptide deformylase, J. Am. Chem. Soc. 127 (2005) 2396.
[24] F. Dardel, S. Ragusa, C.L.S. Blanquet, T. Meinnel, Solution structure of Nickel-Peptide deformylase, J. Mol. Biol. 280 (1998) 501–513.
[25] R.P. Beckett, A.H. Davidson, A.H. Drummond, P. Huxley, M. Whittaker, Recent advances in matrix metalloproteinase inhibitor research, Drug Discov. Today 1 (1996) 16–26.
[26] S.P. East, R.P. Beckett, D.C. Brookings, J.M. Clements, S. Doel, K. Keavey, G. Pain, H.K. Smith, W. Thomas, A.J. Thompson, R.S. Todd, M. Whittaker, Peptide deformylase inhibitors with activity against respiratory tract pathogens, Bioorg. Med. Chem. Lett. 14 (2004) 59–62.
[27] J.M. Clements, R.P. Beckett, A. Brown, G. Catlin, M. Lobell, S. Palan, W. Thomas, M. Whittaker, S. Wood, S. Salama, P.J. Baker, H.F. Rodgers, V. Barymin, D.W. Rice, M.G. Hunter, Antibiotic activity and characterization of BB-3497, a novel Peptide deformylase inhibitor, Antimicrob. Agents Chemother. 45 (2001) 563–570.
[28] J.P. Guilloteau, M. Mathieu, C. Giglione, V. Blanc, A. Dupuy, M. Chevrier, P. Gil, A. Famechon, T. Meinnel, V. Mikol, The crystal structures of four Peptide deformylases bound to the antibiotic actinonin reveal two distinct types: a platform for the structure-based design of antibacterial agents, J. Mol. Biol. 320 (2002) 951–962.
[29] S. Ragusa, P. Mouchet, C. Lazennec, V. Dive, T. Meinnel, Substrate recognition and selectivity of Peptide deformylase. Similarities and differences with metzincins and thermolysin, J. Mol. Biol. 289 (1999) 1445–1457.